Density Perturbations in Polymers Near a Solid Substrate: An X-ray Reflectivity Study

C. Bollinne, V. W. Stone,† V. Carlier, and A. M. Jonas*

Laboratoire de Physique et de Chimie des Hauts Polymères, Université catholique de Louvain, Place Croix du Sud 1, B1348 Louvain-la-Neuve, Belgium

Received March 10, 1999

ABSTRACT: We have studied by X-ray reflectometry the variation of electron density of thin polymer films near solid substrates. For most polymers studied, which interact only mildly with the selected substrate (SiO_2), a decrease of density was detected over a region spanning two to three statistical segment lengths at the solid interface. For poly(4-vinylpyridine) (P4VP), however, an increase of density was observed. This is related to the existence of strong adsorption interactions between P4VP and SiO_2. These observations are in good agreement with theoretical predictions and may play a role in explaining the variation of the glass transition of thin supported polymer films as compared to bulk glass transitions.

Introduction

Understanding the structure and dynamics of polymers near solid walls is important in areas such as polymer processing, lubrication, adhesion, and material properties. Surfaces and interfaces indeed play an important role in modern materials. Many high performances materials contain organic−polymer or inorganic−polymer interfaces. In addition, with the development of nanotechnologies and the increased trend toward miniaturization, the need to understand polymers at interfaces is further increased. This is for instance important for thin and ultrathin polymer films, which are technologically important systems, whose behavior may be dominated by interfacial effects.

Owing to the importance of this topic, numerous studies have concentrated on the perturbations of the dynamical properties of polymers near solid interfaces, either on filled polymers[1−5] or on model systems such as thin films.[6−12] It is beyond the scope of this introduction to review the vast literature on this subject. In contrast, much less experimental work has been devoted to the characterization of static properties of polymers in their condensed state near solid substrates. Although theoretical works have predicted perturbations of polymer chains near solid walls (coil shapes, segment density, radii of gyration, conformations, ...),[13−19] the experimental detection of such perturbations remains elusive. However, such issues may be important to consider before trying to explain the dynamical behavior of polymers near interfaces.

In this paper, we will address experimentally the question of the density evolution of polymers near solid substrates, by determining density profiles on thin polymer films using X-ray reflectometry. Because we are interested in relatively minor perturbations, careful analysis procedures had to be followed. These are described in the Experimental Section. Different anionic polymers of different molecular weights have been used in this study, while the substrate selected is the native silicon oxide layer of a clean silicon wafer.

† Present address: U.C.B. Chemicals S.A., Research and Technology, 33 rue d'Anderlecht, B1620 Drogenbos, Belgium.

Table 1. Characteristics of the Polymers Used in This Study

polymer	molecular mass ($10^3 M_n$)	R_g[a] (Å)	polydispersity index
PMMA	528.4	∼142	1.11
	88.6	∼58	1.03
PS	1030	∼277	1.05
	66	∼70	1.03
P4VP	81.5	∼91	1.18

[a] Radii of gyration were computed from the following statistical segments lengths: $b_{PS} = 6.81$ Å;[20] $b_{PMMA} = 4.88$ Å;[20] $b_{P4VP} = 7.97$ Å.[21]

Experimental Section

Polymers. Polymers used in this study are PS (poly(styrene)), PMMA (poly(methyl methacrylate)) and P4VP (poly(4-vinylpyridine)). PS was obtained from Polymer Laboratories, Church Stretton, U.K. PMMA and P4VP were obtained from Polymer Source Inc., Dorval, Quebec, Canada. Samples used in this study are described in Table 1. These polymers were selected for the potential differences in the way they interact with the substrate considered.

Substrates. The substrates used are silicon wafers with their layer of native oxide (∼13 Å ± 2 Å as measured by ellipsometry), obtained from Wäcker (n-type, ⟨100⟩ orientation). Prior to spin coating, these wafers were cleaned by immersion for 20 min in a freshly made solution [1:1 v/v of sulfuric acid (98%, Merck) and hydrogen peroxide (27%, Vel) (piranha solution)]. The wafers were then thoroughly rinsed in MilliQ water and dried by spinning at 3000 rpm in a clean room environment. This procedure efficiently removes the organic contaminants without introducing measurable roughening of the surface. This cleaning procedure has been reported[22,23] to produce a highly hydrophilic surface by leaving on the silicon oxide layer a relatively dense layer of Si−OH functions.

Preparation of the Samples. The polymer films were prepared by spin coating (speed: 3000 rpm) from polymer solutions of different concentrations directly after having cleaned the substrate, in a clean room environment. In the case of PS and PMMA, the solvent used was toluene (Merck, p.a.). In the case of P4VP, the solvent used was pyridine (Acros, 99+%, spectrophotometric grade). These solvents allow the deposition of smooth and homogeneous films, which is a prerequisite for X-ray reflectometry. To obtain the relationship between film thickness and solution concentration, a series of films were measured by ellipsometry. From these calibrations, we then selected spin-coating concentrations giving thicknesses around $4R_g$ (radius of gyration) for each polymer. This allows minimizing confinement effects on film structure.

10.1021/ma990363n CCC: $18.00
Published on Web 06/22/1999

The samples were measured by XRR before and after annealing. The annealing took place in a vacuum furnace equipped with a trap for oil vapors. The samples were annealed for 5 h at temperatures from 35 to 50 °C above the T_g of the bulk polymer, and then quenched in air at room temperature.

Characterization Techniques

X-ray Reflectivity (XRR). Measurements and Data Reduction. XRR measurements were performed with a $\theta-2\theta$ goniometer (D5000 from Siemens; radius of the goniometer = 30 cm), which is mainly composed of a Cu K$\bar{\alpha}$ source (λ = 1.5418 Å), a graphite secondary monochromator, a scintillation counter, and a Siemens reflectometry stage modified in house. The divergence of the beam in the incidence plane was set by a variable 1 μm precision slit; typical divergences of 0.0084° were used. The reflected beam was collected through a 200 μm wide detector slit. Soller slits in the incident and reflected beam limited axial divergence to 0.02°. A special automated alignment procedure allowed the sample to be positioned within a few micrometers from the goniometer sample.[24] The incident intensity and reflected intensity at low angles of incidence were measured through a calibrated filter to avoid overexposure of the detector.

The reflected intensity was divided by the measured incident intensity to obtain reflectivity. The data were corrected for background scattering and invariance of the illuminated area at very low angles of incidence (below ≅0.125°, depending on sample size). The data are reported as a function of k_{z0}, the component perpendicular to the interface of the wavevector in vacuum of the incident photons ($k_{z0} = (2\pi/\lambda)(\sin\theta)$, where λ is the X-ray wavelength and θ is half the angle between incoming and outgoing beams).

XRR Data Analysis. The data were analyzed by an iterative procedure performed in reciprocal and real space. The procedure is based

- on the comparison between measured reflectivity and reflectivity computed from a density profile to be optimized;
- on the comparison between an experimental correlation function and the correlation function computed from the simulated reflectivity.

The correlation function used is the self-correlation of the derivative of the electron density profile $\rho(z)$, which is defined as

$$P(r) = \frac{1}{\rho_s^2}\int_{-\infty}^{+\infty}\frac{d\rho(z)}{dz}\frac{d\rho(z+r)}{dz}\,dz \qquad (1)$$

where ρ_s is the electron density of the substrate.

Under the validity conditions of the first Born approximation, this function can be computed from reflectivity data ($R(k_z)$), by means of a Fourier transform:[25−27]

$$P_R(r) = \frac{1}{2\pi}\int_{-\infty}^{+\infty}\frac{R(k_{z1})}{R_F(k_{z1})}\exp(2ik_{z1}r)\,dk_{z1} \qquad (2)$$

where k_{z1} is the component perpendicular to the interface of the wave vector *in the film* (i.e. we operate a refraction correction as suggested by others[28,29]) and $R_F(k_{z1})$ is the Fresnel reflectivity of the bare and perfectly smooth substrate computed at k_{z1}.

Since the first Born approximation is not valid near the critical angle for total external reflection, $P_R(r)$ is not strictly equal to $P(r)$. We thus call $P_R(r)$ the *pseudo*autocorrelation function.

The construction of the density profile from the reflectivity data was done in the following way. We first select an a priori model for the density profile, consisting in one layer, which describes the film as a continuous slab of constant density. We calculate the reflectivity associated with this particular model using Parrat's formalism,[30] and adjust the different parameters (thickness, roughness, and electron density) of the slab and substrate, to minimize

$$\chi^2 = \sum_{j=1}^{N}\left(\frac{R_{meas,j} - R_{calc,j}}{w_j}\right)^2 \qquad (3)$$

where $R_{meas,j}$ is the measured reflectivity, $R_{calc,j}$ is the computed reflectivity and w_j is a weight equal to the standard error on point j. At this stage of the process, if the control parameter χ^2 has an acceptable value, we stop the fit. We then calculate and compare $P_R(r)$, computed from fit and $P_{R,exp}(r)$, computed from the experimental data. Note that we do not compare directly the self-correlation of the electron density, $P(r)$, with $P_{R,exp}(r)$, since these two functions always differ slightly due to the failure of the first Born approximation at very low angles. Because the Fourier transform in eq 2 has the virtue to accumulate at the same spatial location small periodic differences between R_{meas} and R_{calc}, the comparison between $P_R(r)$ and $P_{R,exp}(r)$ reveals clearly such differences that are not easily detectable in reciprocal space. The comparison between $P_R(r)$ and $P_{R,exp}(r)$ is performed qualitatively: all the features (peaks, valleys) of $P_{R,exp}(r)$ must be found in $P_R(r)$. If the agreement between the two functions is qualitatively good and χ^2 is low enough, we stop the adjustment procedure. The obtained density profile is, following a very good probability, the most appropriate to describe the structure of the film, perpendicular to its surface.

If χ^2 is too high and/or the shapes of $P_R(r)$ and $P_{Rexp}(r)$ show noticeable differences, we restart the fitting procedure with a more complex model for the density profile. That is to say we introduce one or two more layers, at locations suggested by the examination of $P_{R,exp}(r)$, usually at the interfaces. These layers do not have a physical meaning as such but have as a goal to introduce a perturbation (by comparison to the initial homogeneous layer) in the density profile. Again, we fit the parameters and compare $P_R(r)$ and $P_{Rexp}(r)$. This procedure is repeated with more and more complex models (e.g. obtained by dividing each layer situated at the interfaces in two) till we have together a low value for χ^2 and a qualitatively good agreement between $P_R(r)$ and $P_{Rexp}(r)$. If these conditions are fulfilled for models containing an important number of layers (more than six), we try finally to simplify this model in order to keep the main features of the density profile, while reducing the number of parameters. In some instances we found it useful to use a regularization technique during the fits, as described elsewhere.[31]

Results

PS. We present in Figure 1 the XRR data pertaining to sample PS 66k, together with a fit using a simple model (homogeneous film of ∼320 Å thickness). Although the fit reproduces quite well the data in reciprocal space (Figure 1a), the comparison between $P_R(r)$ and $P_{R,exp}(r)$ (Figure 1b) reveals a major difference in real space: the simulation clearly lacks a dip in the region 15 Å < r < 50 Å. This indicates that the model should include a density fluctuation near one of its interface. Because of the symmetry properties of autocorrelation functions, one can envision two possibilities, either a decrease of density near the substrate or a density excess near the free interface. The latter possibility can be safely excluded, as being unrealistic. In addition, this selection could not explain the results obtained on other samples (see below).

Figure 2 presents the fits and pseudocorrelation functions obtained with a more complex model, in which we have added two supplementary layers, one at the substrate interface and one at the free interface. The best fit coincides with a model where the electron density of the film decreases near the substrate interface, as shown in the inset of Figure 2a. The pseudocorrelation functions now show a much better agreement (Figure 2b), with all the features of $P_{R,exp}(r)$ being

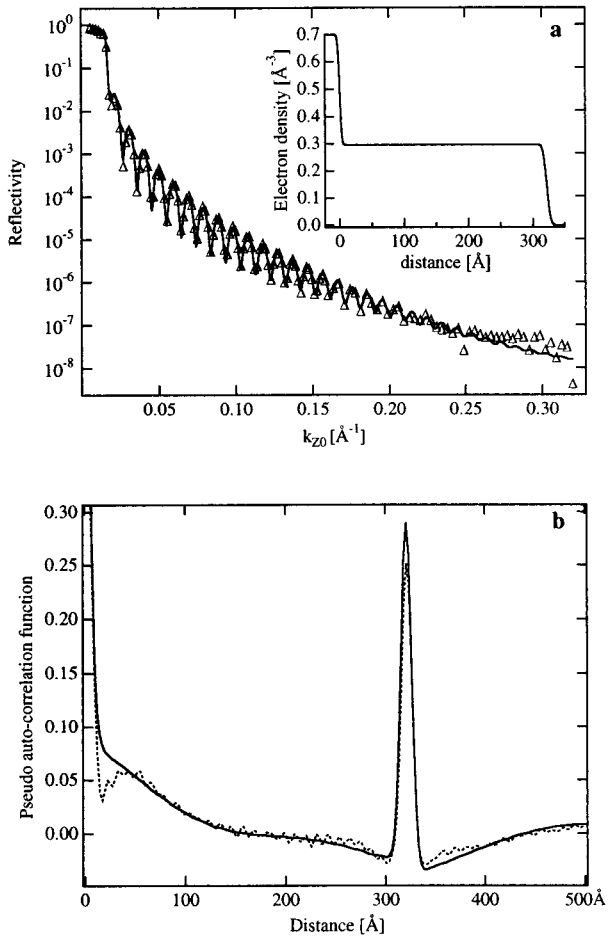

Figure 1. (a) X-ray reflectogram, fit (one-layer model), and density profile for PS 66k. The film was measured after annealing during 5 h, at 150 °C. For the clarity of the figure, only every fifth point has been represented in the reflectogram. (b) Pseudoautocorrelation function calculated from the experimental data (dashed line) and from the fit (continuous line).

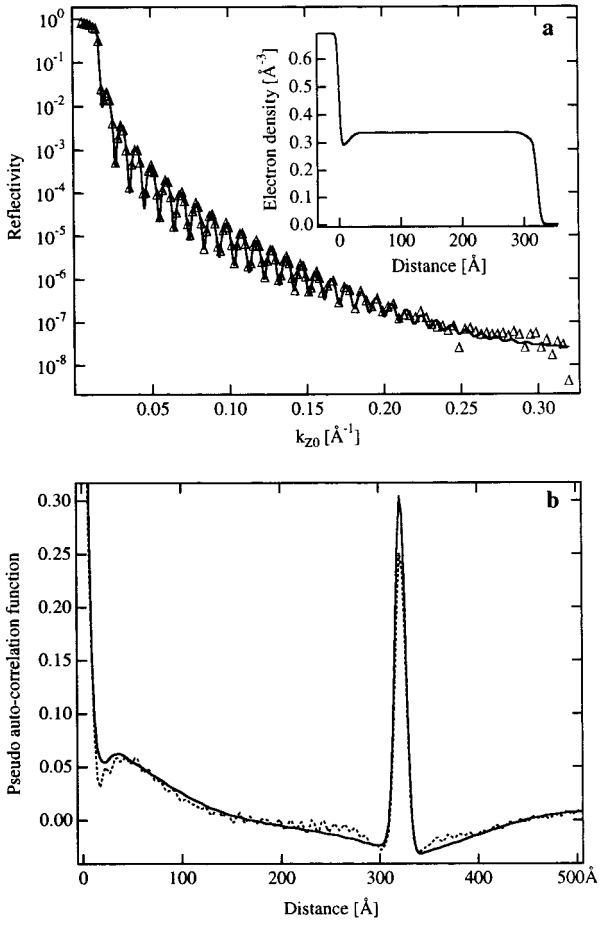

Figure 2. (a) X-ray reflectogram, fit (three-layers model), and density profile for PS 66k. The film was measured after annealing during 5 h, at 150 °C. For the clarity of the figure, only every fifth point has been represented in the reflectogram. (b) Pseudoautocorrelation function calculated from the experimental data (dashed line) and from the fit (continuous line).

reproduced by $P_R(r)$: the main peak due to the correlation between the two interfaces near 320 Å and the depression of $P_R(r)$ near the origin, due to the dip in electron density at the substrate interface. Note that the roughness of the free interface differs also slightly from a pure Gaussian roughness, as can be detected by comparing the insets of Figure 1a and of Figure 2a.

We have estimated the extent and the dimension of the perturbation of density near the substrate by computing the integral width (w_d) and surface (A_d) of the dip, using as baseline the film electron density far away from the substrate (ρ_f), as reported in Table 2. Also reported are the values found for a PS having 1030k as molecular mass (data not shown in the paper). It is important to realize that the precision on these parameters is low, due to the limited sensitivity of XRR to the exact shape of the density perturbation at the interface. As can be seen in Table 2, the characteristics of the dip are not significantly modified when increasing the molecular mass by a factor of about 15.

P4VP. We then determined the density profile and the pseudocorrelation function of a film of poly(4-vinylpyridine) (P4VP) spin-coated onto Si/SiOx. As before, we used two models to fit the data: a simple homogeneous film (Figure 3) and a more complex model (Figure 4) by introducing one or more thin layers near the two interfaces. In contrast to PS, a denser layer had to be introduced near the solid interface in order to fit correctly the experimental data, in the reflectivity profile and in the pseudocorrelation function (compare Figure 3 with Figure 4). The height and extent of this bump are reported in Table 2. The spatial extent of this bump is somewhat higher than what was found for the density depletion in PS.

Table 2. Integral (A_d) and Integral Width (w_d) of the Density Modification near the Substrate[a]

polymer	A_d (Å^{-2})	w_d (Å)
PS 66k	−0.66	15.0
PS 1030k	−0.37	12.2
PMMA 88.6k	−0.28	13.3
PMMA 528.4k	−0.61	11.7
P4VP 81.5k	+0.58	26.9

[a] Positive values of A_d indicate an increased density near the substrate, while negative values indicate a depletion.

PMMA. The same procedures were applied to analyze PMMA films spin-coated onto Si/SiOx. Here, we simply present the results obtained for fits with the finally selected models in Figure 5 for PMMA 88.6k. As for PS, the introduction of a dip in the electron density profile near the substrate was found necessary to allow a complete reproduction of the experimental data in reciprocal and direct spaces. These dips were found to be slightly comparable in their spatial extents and in their amplitudes to those of PS films (see Table 2).

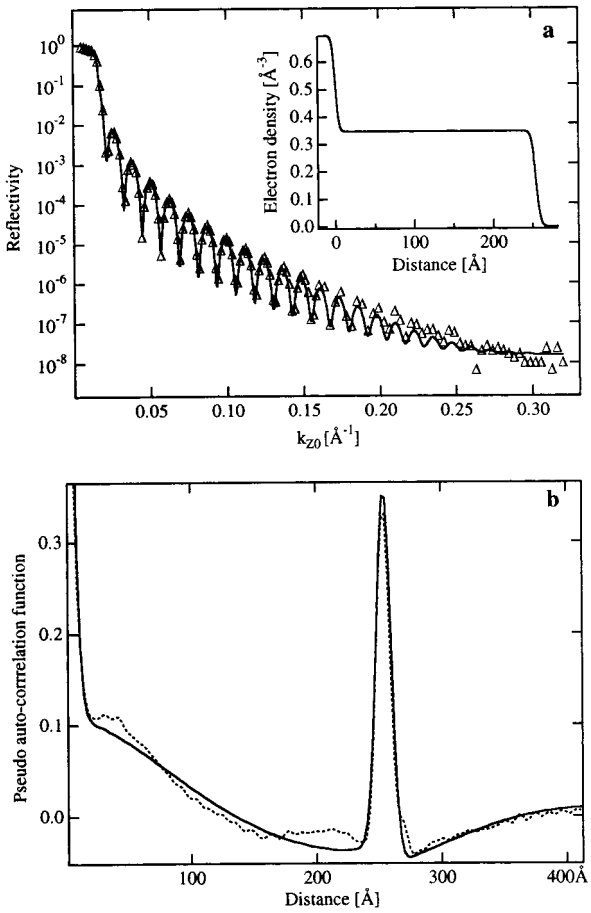

Figure 3. (a) X-ray reflectogram, fit (one-layer model), and density profile for P4VP 81.5k. The film was measured after annealing during 5 h, at 190 °C. For the clarity of the figure, only every fifth point has been represented in the reflectogram. (b) Pseudoautocorrelation function calculated from the experimental data (dashed line) and from the fit (continuous line).

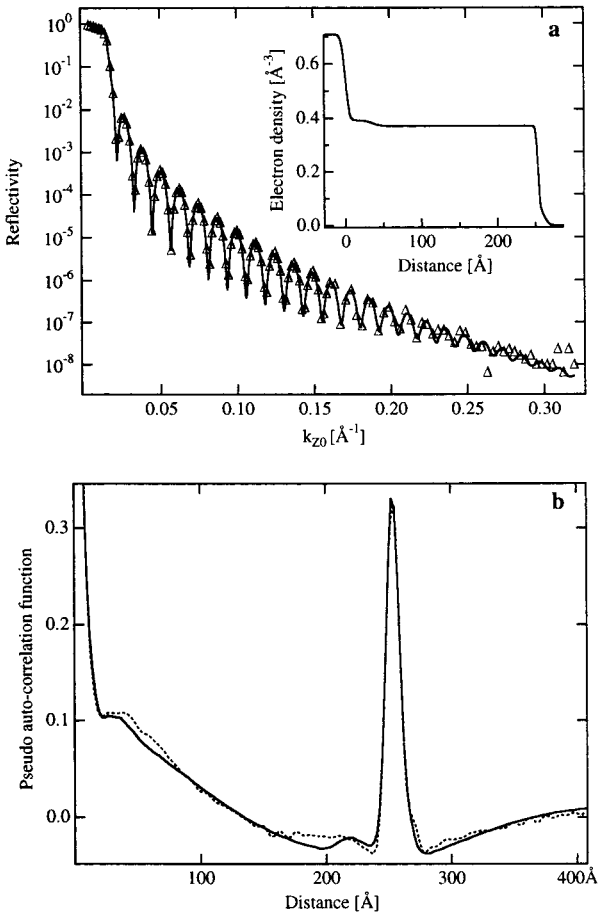

Figure 4. (a) X-ray reflectogram, fit (three-layers model), and density profile for P4VP 81.5k. The film was measured after annealing during 5 h, at 190 °C. For the clarity of the figure, only every fifth point has been represented in the reflectogram. (b) Pseudoautocorrelation function calculated from the experimental data (dashed line) and from the fit (continuous line).

One should note that similar dips were found by us necessary to reproduce the X-ray reflectograms of a series of other polymers spin-coated onto Si/SiOx: chlorinated poly(butadiene),[24] poly(methyl hexyl silylene),[32] atactic poly(propylene),[32] and chlorinated poly(propylene).[32] Also, it should be mentioned that this was found true for measurements performed with two different reflectometers, differing in their X-ray source and beam collimation systems, and for films produced by different persons in different environmental conditions. Finally, it is important to mention that such dips were not found when analyzing polyelectrolyte multilayers deposited by self-assembly onto similar Si/SiOx substrates.[33] This effectively rules out the possibility that the reported density perturbations be due to an improper handling of the substrates after cleaning, or to artifacts in our analysis methods.

Discussion

For the different systems analyzed in this study, local perturbations of the density profile were observed near the substrate interface (either a depletion or an increase). The reproducibility of our experiments and the quantitative differences observed between P4VP and PS exclude the possibility that our observations be due to artifacts or surface contamination. Therefore, their origin should be sought in a variation of the free volume (excess or depletion) near the substrate. Perturbations of the macromolecular conformations near the substrate are the most probable cause for these density fluctuations. Indeed, several simulations and theoretical works predict a perturbation of the local segmental distribution near surfaces: a decrease of density is expected for nonadsorptive surfaces,[15,34] while an increase of density is predicted for strongly adsorptive surfaces.[15,17,34] According to these studies, the density perturbations near a solid wall span a distance of about two statistical segment lengths and depend on the strengths of the surface-monomer potential. Except for P4VP, where the experimental integral width of the density modification is slightly larger than three statistical segment lengths (Table 2), the experimental integral widths of the density perturbations are indeed about two statistical segment lengths, which is in good agreement with theoretical predictions. The independence of this width with molecular weight is also in agreement with the predicted localized nature of the density perturbations, which do not scale with the radius of gyration of the statistical coil. Finally, the strength of the density perturbations (Table 2) evolves qualitatively consistently with the strength of the surface−monomer potential. Indeed, interactions between PS and silicon oxide (a polar substrate and a nonpolar polymer) are weak, and the monomer−surface potential is dominated by weak nonadsorptive van der Waals interactions. Accordingly, a depletion of density near the substrate is observed. In contrast, P4VP is capable to develop

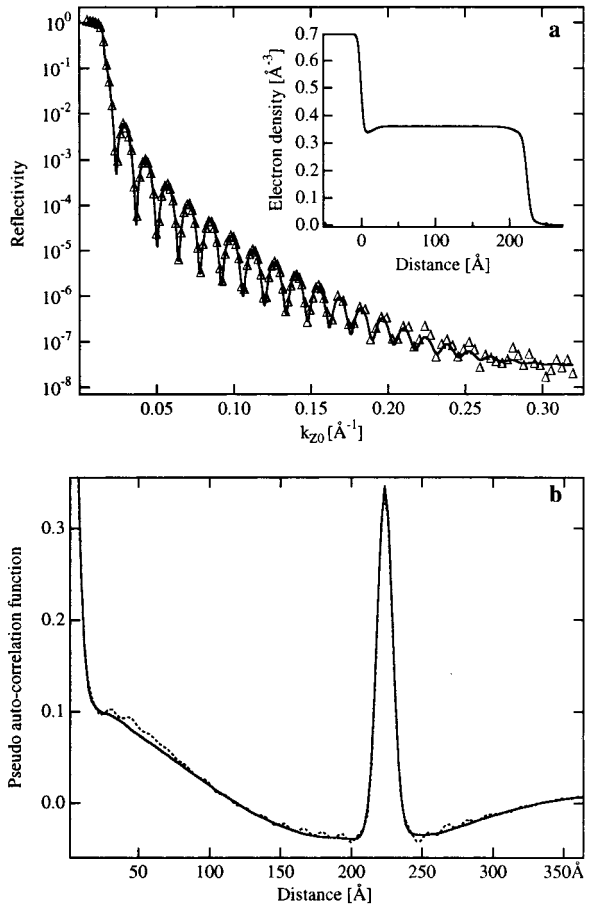

Figure 5. (a) X-ray reflectogram, fit (three-layers model), and density profile for PMMA 88.6k. The film was measured after annealing during 5 h, at 150 °C. For the clarity of the figure, only every fifth point has been represented in the reflectogram. (b) Pseudoautocorrelation function calculated from the experimental data (dashed line) and from the fit (continuous line).

acid−base interactions with the acidic silicon oxide surface. Accordingly, density increases near the interface. The behavior of PMMA would be expected to be intermediate between PS and P4VP, since PMMA interacts mildly with silicon oxide, with possible hydrogen bonds between PMMA and silicon oxide being weaker than acid−base interactions but stronger than purely dispersive van der Waals interactions. However, due to the limited sensitivity of XRR, we were not able to detect significant differences between PMMA and PS in this study. Other experimental techniques should be used to distinguish PMMA from PS.

Recently, a lot of work has been dedicated to the study of dynamical properties of thin polymer films, more particularly to the determination of the glass transition temperature (T_g) or the dewetting temperature of thin polymer films.

For PS films deposited onto passivated silicon, Keddie et al.[6,7] showed that the T_g of the films decreased with thickness, by comparison with the bulk T_g of the same polymer. It has also been shown[6] that when PMMA is deposited onto silicon wafer coated with native oxide, the T_g of the polymer films slightly increases above the bulk T_g value, depending on film thickness. van Zanten et al.[10] have observed an increase in the T_g of P2VP (up to 50 K above the bulk T_g), for films thinner than the radius of gyration of the unperturbed chain (R_g) deposited onto silicon oxide. It is interesting to note that the importance of the perturbations of T_g in thin films have some similarity with the density perturbations detected in the present paper. Since we know the importance of free volume with respect to T_g, it may be that these density perturbations are in part responsible for the reported T_g variations.

Conclusions

XRR studies of different polymer films (PS, PMMA, P4VP) deposited onto silicon wafers covered with their native oxide indicate perturbations of the density profile near the solid substrate, either a depletion (PS, PMMA) or an increase of density (P4VP). The importance of these effects correlates with the strength of the interactions developed between the polymer and silicon oxide, weak and nonadsorptive in the case of PS and strong and adsorptive in the case of P4VP. The limited sensitivity of XRR did not allow us, however, to reveal differences between PS and PMMA. The presence of these thin layers of modified density near the substrate was supported by the calculation of the pseudoautocorrelation functions. The determination of these functions is directly based on the experimental data and is therefore not affected by fitting artifacts. The spatial extent of these perturbations spans two to three statistical segment lengths and is independent of the molecular weight of the polymer. These observations are in relatively good agreement with earlier theoretical predictions.[17,34] We suggest that such perturbations may be responsible in part for the variations of T_g detected in thin polymer films as compared to bulk polymers.

Acknowledgment. Partial financial support of this work by the Belgian Fund for Scientific Research (FNRS) is gratefully acknowledged. C. Bollinne acknowledges financial support by the "Fonds Spéciaux de Recherche" (FSR, UCL) and the "Fonds pour la Formation à la Recherche dans l'Industrie et l'Agriculture" (FRIA). The authors wish to thank X. Arys for his contribution to the development of procedures of reflectivity analysis in our lab.

References and Notes

(1) Tsagaropoulos, G.; Eisenberg, A. *Macromolecules* **1995**, *28*, 6067.
(2) Tsagaropoulos, G.; Eisenberg, A. *Macromolecules* **1995**, *28*, 396.
(3) Isaka, K.; Shibayama, K. *J. Appl. Polym. Sci.* **1978**, *22*, 3135.
(4) Thomason, J. L. *Composites Sci. Technol.* **1992**, *44*, 87.
(5) Sclavons, M.; Carlier, V.; Legras, R. In *Proceedings of the 1st International Conference on Composites Engineering (ICCE/1)*; New Orleans, LA, August 28−31, 1994; Hui, D., Ed.; New Orleans, LA, 1994; pp 931−932.
(6) Keddie, J. L.; Jones, R. A. L.; Cory, R. A. *Faraday Discuss.* **1994**, *98*, 219.
(7) Keddie, J. L.; Jones, R. A. L.; Cory, R. A. *Europhys. Lett.* **1994**, *27*, 59.
(8) Reiter, G. *Europhys. Lett.* **1993**, *23*, 579.
(9) Reiter, G. *Macromolecules* **1994**, *27*, 3046.
(10) van Zanten, J. H.; Wallace, W. E.; Wu, W.-L. *Phys. Rev. E* **1996**, *53*, 2053.
(11) Forrest, J. A.; Dalnoki-Veress, K.; Stevens, J. R.; Dutcher, J. R. *Phys. Rev. Lett.* **1996**, *77*, 2002.
(12) Forrest, J. A.; Dalnoki-Veress, K.; Dutcher, J. R. *Phys. Rev. E* **1997**, *56*, 5705.
(13) Theodorou, D. N. *Macromolecules* **1988**, *21*, 1391.
(14) Theodorou, D. N. *Macromolecules* **1988**, *21*, 1400.
(15) Theodorou, D. N. *Macromolecules* **1989**, *22*, 4589.
(16) Mansfield, K. F.; Theodorou, D. N. *Macromolecules* **1989**, *22*, 3143.
(17) Mansfield, K. F.; Theodorou, D. N. *Macromolecules* **1991**, *24*, 4295.
(18) Kumar, S. K.; Vacatello, M.; Yoon, D. Y. *Macromolecules* **1990**, *23*, 2189.

(19) Yethiraj, A.; Hall, C. K. *Macromolecules* **1990**, *23*, 1865.
(20) Sato, M.; Koshiishi, Y.; Asahina, M. *Polym. Lett.* **1963**, *1*, 233.
(21) Computed from data in: Yoshida, M.; Sakamoto, N.; Ikemi, K.; Arichi, S. *Bull. Chem. Soc. Jpn.* **1992**, *65*, 3108.
(22) Elman, J. F.; Johs, B. D.; Long, T. E.; Koberstein, J. T. *Macromolecules* **1994**, *27*, 5341.
(23) Carim, A. H.; Dovek, M. M.; Quate, C. F.; Sinclair, R.; Vorst, C. *Science* **1987**, *237*, 630.
(24) Stone, V. W. Ph.D. Thesis, Université catholique de Louvain, 1999.
(25) Russell, T. P. *Mater. Sci. Rep.* **1990**, *5*, 171.
(26) Sivia, D. S.; Hamilton, W. A.; Smith, G. S.; Rieker, T. P.; Pynn, R. *J. Appl. Phys.* **1991**, *70*, 732.
(27) Als-Nielsen, J. *Physica* **1984**, *126B*, 145.
(28) Bridou, F.; Pardo, B. *J. Phys. III Fr.* **1994**, *4*, 1523.
(29) Toney, M. F.; Thompson, C. *J. Chem. Phys.* **1991**, *92*, 3781.
(30) Parrat, G. *Phys. Rev.* **1954**, *95*, 359.
(31) Petersen, J. K.; Hamley, I. W. *J. Appl. Crystallogr.* **1994**, *27*, 36.
(32) Bollinne, C. Unpublished results.
(33) Arys, X.; Jonas, A. M.; Laguitton, B.; Legras, R.; Laschewsky, A.; Wischerhoff, E. *Prog. Org. Coat.* **1998**, *34*, 108.
(34) Bitsanis, I. A.; ten Brinke, G. *J. Chem. Phys.* **1993**, *99*, 3100.

MA990363N